Research Paper

Volume : 3 | Issue : 5 | May 2014 • ISSN No 2277 - 8179

Robust Dynamic Inverse Controller For Spacecraft Model

Engineering

KEYWORDS : Dynamic inverse, Robust control, Spacecraft

Settar S. Keream	Faculty of Elect and Electronic Engineering, University Malaysia Pahang, Pekan 26600, Malaysia
Ahmed N Abdalla	Faculty of Elect and Electronic Engineering, University Malaysia Pahang, Pekan 26600, Malaysia
Ruzlaini Ghoni	Faculty of Elect. Auto. Eng. Tech., TATi Malaysia, University College, Kemaman 24000,
Mohd Razali Daud	Faculty of Elect and Electronic Engineering, University Malaysia Pahang, Pekan 26600, Malaysia
Youssif Al Mashhadany	University of Anbar, Dept. of Electrical Engineering College, Anbar, Iraq

ABSTRACT

typically, the spacecraft model has high uncertainties and the dynamic inverse inner loop controller alone may not achieve acceptable performance. Therefore, a robust outer loop must be added to compensate this inner-loop deficit. In this paper, a robust controller based on dynamic inverse technique for proto type vehicle X-38 model was proposed. The controller contains two loops. The inner loop is dynamic inverse controller which cancels existing system dynamics and replaces them with designer specified response, and the outer loop is a Linear Quadratic Gaussian (LQG) which is used as a robust approach. Several forms of desired dynamic are presented and evaluated in terms of performance and robustness including a proportional dynamics, proportional integral dynamics, flying quality dynamics and ride quality dynamics. The simulation results shows that flying quality and ride quality have been used as a desired dynamics. The ride quality has been proved to be more robust, then the other desired dynamics, against wide range of system parameter variation.

INTRODUCTION

The dynamic inversion is a technique that has been widely studied and applied in many field in army and industry. Comprehensive and rigorous proofs for transforming a nonlinear system into an equivalent linear system (called either feedback linearization or dynamic inversion and based on the early papers [1-2]). At about the same time theoretical advances have essentially completed the background for insuring feedback control laws which make prescribed outputs independent of important classes of inputs, namely disturbances and decoupled control effectors.

These two important aspects of control theory non-interacting control laws and transformation of nonlinear systems into equivalent linear ones are embodied in what is now often called "dynamic inversion". In [3] presents a Decoupling in the Design and Synthesis of Multivariable Control Systems; consider non-interactions as a facet of linear systems theory. In [4] extend these notions to nonlinear systems, Decoupling in a Class of Nonlinear Systems by State Variable Feedback. In [5] made a significant contribution to dynamic inversion theory with mathematical notions from differential geometry.

An approach for the exact dynamic inversion of singularly perturbed second-order linear systems through asymptotic expansion in a singular parameter has been proposed by (Cheong et al., 2012.[6]). Results showed that the inversion solution, corresponding to the invariant slow manifold, can be expressed as a converging infinite series under desired output constraints composed of exponential support functions in the complex domain. It can be seen the providing systematic mathematical procedures to obtain the closed-form invariant slow manifold, along with required admissible boundary conditions.

An inverse dynamics solution for a given tip trajectory with given initial conditions has been introduced by (Mandali et al., 2011). Balas [7] and his colleagues have applied these ideas to a variety of aerospace flight control system designs – including the F-18 High Angle-of-Attack Research Vehicle (HARV) and the X-38 itself. They have also provided powerful software tools that are commercially available and widely used by control design practitioners. Thus, there is no doubt that the mathematical tools and the underlying theory is available to both industry and to government agencies. However, there are open issues as to the practicality of using dynamic inversion as the only (or even the primary) design approach for reentry vehicles.

In this paper, design the dynamic inverse by using the simple procedure for X-38 model. Various aspects of system performance were discussed and illustrated by simulation results. For proportional and proportional integral cases, the system fails to satisfy the limitation imposed on aileron deflection rate and rudder deflection rate. The flying quality and ride quality can satisfy all the requirements. However, ride quality can satisfy faster response with acceptable deflection and rate of deflection in aileron and rudder.

DYNAMIC INVERSION CONCEPT (LINEAR AIRCRAFT CONTROLLER)

DI is a controller synthesis technique by which existing deficient or undesirable dynamics are canceled and replaced by designer-specified desirable dynamics. This cancellation and replacement are accomplished by careful algebraic selection of a feedback function. It is for this reason that the DI methodology is also called feedback linearization [7].

The block diagram representation of DI control concept is illustrated in Figureure.(1) where CV represents a user-defined control variable. A fundamental assumption in this approach is that the plant dynamics are perfectly modeled, and therefore can be canceled exactly by the feedback functions. In practice this assumption is not realistic; the DI controller requires some level of robustness to suppress undesired behavior due to plant uncertainties. To overcome this potential robustness problem, many studies employ singular value (μ)- synthesis to create a robust outer loop for the DI controller [7,8]. The aircraft dynamics are expressed by

$$\dot{x} = F(x,u) \qquad (1)$$
$$y = H(x)$$

Where x is the state vector and u is the control vector; y is the output vector. For conventional (small perturbations from trim conditions) the function F is linear in u. Eq.1 can also be re-

written as

$$\dot{x} = f(x) + g(x)u \qquad (2)$$

Where f is a nonlinear state dynamic function and g is a nonlinear control distribution function [9]. If we assume g(x) is invertible for all values of x, the control law is obtained by subtracting f(x) from both sides of eq.2 and then multiplying both sides by g-1(x).

$$u = g^{-1}(x)[\dot{x} - f(x)] \qquad (3)$$

The next step is to command the aircraft to specified states instead of specifying the desired states directly, we specify the rate of the desired states, $\dot{x}$. By swapping $\dot{x}$ in the previous equation to $\dot{x}_{des}$, it get the final form of a dynamic inversion control law:

$$u = g^{-1}(x)[\dot{x}_{des} - f(x)] \qquad (4)$$

Figure. 2 shows the block diagram representation of the DI process.

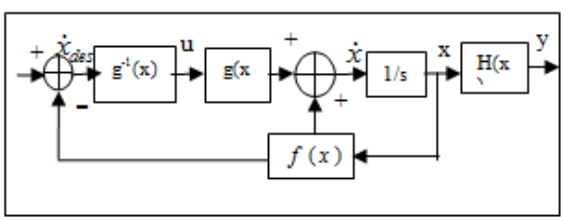

Figure. 1: Dynamic inversion process

Even though the basic dynamic inversion process is simple, there are a few points to be emphasized.

First, we assume g(x) is invertible for all values of x. However, this assumption is not always true. For example, g(x) is not generally invertible if there are more states than there are controls. Furthermore, even if g(x) is invertible (for example: g(x) is small), the control inputs, u, become large and this growth are a concern because of actuator saturation. Since the dynamics of the actuators, as well as sensor noise in the feedback loop [10], are also neglected during this primitive controller development to illustrate the process, a "perfect" inversion is not possible.

Dynamic Inversion is also essentially a special case of model-following. Similar to other model-following controllers, a DI controller requires exact knowledge of the model dynamics to achieve a good performance. To overcome these difficulties, a DI controller is normally used as an inner loop controller in combination with an outer loop controller, which is designed using other control design techniques.

The closed loop transfer function for a desired control variable, CV, being inverted is found according to Figure.2. From this block diagram, it is observed that the desired dynamics operate on the error between the commanded CV and its feedback term, as shown on the block diagram [10].

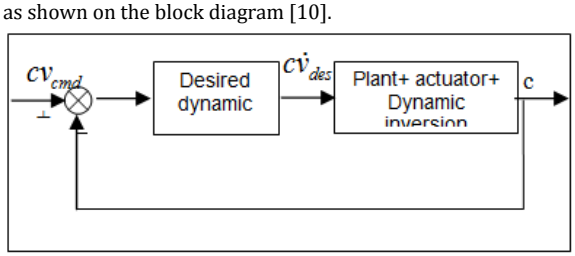

Figure. 2: Block Diagram of closed loop transfer function.

SIMPLIFIED LATERAL DIRECTIONAL CONTROLLER FOR AN AIRCRAFT

The X-38, vehicle for the Crew Return Vehicle (CRV), was under development at NASA's\ Johnson Space Center and Dryden Flight Research Center with collaboration from the European Space Agency. This vehicle serves as a "lifeboat" in the event of an emergency on the International Space Station. It has a unique lifting body shape patterned after the X-24A [7]. It has highly nonlinear physical descriptions of the motion which are the subject of these guidelines. These guidelines are to specifically address the needs for re-entry vehicles that must operate, as the X-38 does, through re-entry from space to a controlled touchdown on the surface of the earth. The latter part of this controlled descent may be by parachute or paraglider – or it may be an automatic or human-controlled landing similar to the Shuttle orbiter. Since any crewmembers aboard the vehicle are assumed to be incapacitated, the X-38 flight controller must guide the vehicle autonomously from low earth orbit until deployment of a parafoil during the last minutes of flight [7]. Since the flight envelope of this vehicle extends from hypersonic conditions down to the subsonic regime, its flight controller must deal with large changes in flight conditions.

The linearized Lateral/Directional dynamic equations of the X-38 model are [11]:

$$\begin{bmatrix} \dot{\beta} \\ \dot{p} \\ \dot{r} \\ \dot{\phi} \end{bmatrix} = \begin{bmatrix} \frac{\gamma_\beta}{v_T} & \frac{\gamma_p}{v_T} & \left(\frac{\gamma_p}{v_T} - 1\right) & \frac{g}{v_T} \\ L_\beta & L_p & L_r & 0 \\ N_\beta & N_p & N_r & 0 \\ 0 & 1 & 0 & 0 \end{bmatrix} \begin{bmatrix} \beta \\ p \\ r \\ \phi \end{bmatrix} + \begin{bmatrix} 0 & \frac{\gamma_{\delta r}}{v_T} \\ L_{\delta a} & L_{\delta r} \\ N_{\delta a} & N_{\delta r} \\ 0 & 0 \end{bmatrix} \begin{bmatrix} \delta a \\ \delta r \end{bmatrix} \qquad (5)$$

The Lateral/Directional Dynamic Inversion control equations are developed in this section. However, we now need to simultaneously deal with two states, roll rate and yaw rate, controlled by two control surfaces, ailerons and rudders, instead of one state, pitch rate, controlled by one control surface, elevator, as in the simplified longitudinal case Simplified linear lateral aircraft equations can be written with respect to roll as well as yaw axes as:

$$\dot{p} = L_p p + L_r r + L_\beta \beta + L_{\delta a}\delta a + L_{\delta r}\delta r$$
$$\dot{r} = N_p p + N_r r + N_\beta \beta + N_{\delta a}\delta a + N_{\delta r}\delta r \qquad (6)$$

Writing Eq. 6 in a compact matrix form:

$$\begin{bmatrix} \dot{p} \\ \dot{r} \end{bmatrix} = \begin{bmatrix} L_p & L_r & L_\beta \\ N_p & N_r & N_\beta \end{bmatrix} \begin{bmatrix} p \\ r \\ \beta \end{bmatrix} + \begin{bmatrix} L_{\delta a} & L_{\delta r} \\ N_{\delta a} & N_{\delta r} \end{bmatrix} \begin{bmatrix} \delta a \\ \delta r \end{bmatrix} \qquad (7)$$

Comparing the matrix form of Eq.2 to Eq.7, each parameter is either a vector or a matrix, but the form remains the same.

$$\dot{x} = \begin{bmatrix} \dot{p} \\ \dot{r} \end{bmatrix} \qquad (8)$$

$$x = \begin{bmatrix} p \\ r \\ \beta \end{bmatrix}$$

$$u = \begin{bmatrix} \delta a \\ \delta r \end{bmatrix}$$

$$f = \begin{bmatrix} L_p & L_r & L_\beta \\ N_p & N_r & N_\beta \end{bmatrix}$$

$$g = \begin{bmatrix} L_{\delta a} & L_{\delta r} \\ N_{\delta a} & N_{\delta r} \end{bmatrix}$$

Notice here that the control distribution matrix, g, is a square matrix. Therefore, its inverse exists in general. As a next step, we invert the roll rate and yaw rate dynamic equations to obtain aileron and rudder deflection angles.

Volume : 3 | Issue : 5 | May 2014 • ISSN No 2277 - 8179

$$\begin{bmatrix}\delta a\\ \delta r\end{bmatrix}=\begin{bmatrix}L_{\delta a} & L_{\delta r}\\ N_{\delta a} & N_{\delta r}\end{bmatrix}^{-1}\left\{\begin{bmatrix}\dot{p}\\ \dot{r}\end{bmatrix}-\begin{bmatrix}L_p & L_r & L_\beta\\ N_p & N_r & N_\beta\end{bmatrix}\begin{bmatrix}p\\ r\\ \beta\end{bmatrix}\right\} \quad (9)$$

Then, substituting the desired states $\dot{p}_{des}$ and $\dot{r}_{des}$ for $\dot{p}$ and $\dot{r}$ along with the measured values of p, r and β (pmeas, rmeas and βmeas) for p, r and β, we get the lateral dynamic inversion control law:

$$\begin{bmatrix}\delta a\\ \delta r\end{bmatrix}^{cmd}=\begin{bmatrix}L_{\delta a} & L_{\delta r}\\ N_{\delta a} & N_{\delta r}\end{bmatrix}^{-1}\left\{\begin{bmatrix}\dot{p}\\ \dot{r}\end{bmatrix}^{des}-\begin{bmatrix}L_p & L_r & L_\beta\\ N_p & N_r & N_\beta\end{bmatrix}\begin{bmatrix}p\\ r\\ \beta\end{bmatrix}^{meas}\right\} \quad (10)$$

CONTROL ACTUATOR MODELING

Control surface actuators are modeled with the following second order lag for both rudders and body flaps [11]:

$$G_{act}=\frac{w_n^2}{s^2+2\zeta w_n+w_n^2} \quad (11)$$

Where: wn = 26 rad /sec and ζ= 0.707 in both sets of actuators.

CONTROL SURFACE LIMITS

X-38 control surface deflection limits are listed in Table 1.

TABLE 1. X-38 CONTROL SURFACE DEFLECTION LIMITS

Body flap Lower Deflection Limit (δa)	0.0 º
Body flap Upper Deflection Limit (δa)	45.0 º
Rudder Lower Deflection Limit (δr)	-25.0 º
Rudder Upper Deflection Limit (δr)	25.0 º

Although the actual rate limits of the actuators used for the X-38 vehicle are set as a function of the hinge moment, constant values shown in Table 2 are used for this study.

TABLE 2. X-38 CONTROL SURFACE RATE LIMITS

Body flap Deflection Rate Limit $\dot{\delta}_a$	50 º/sec
Rudder Deflection Rate Limit $\dot{\delta}r$	50 º/sec

PROPOSED MODEL

The Dynamic Inversion control laws developed in previous sections are now integrated into an overall control structure [11]. As the block diagram in Figure. 4 shows, DI control is used as an inner loop accompanied by α and Φ feedback outer loops. Any type of control technique can be used for the outer loop. However, simple feedback is used in this particular example to illustrate the characteristics of the inner loop DI control. The overall DI controller requires commanded values of angle-of-attack,αcmd, and bank angle, Φcmd, as inputs. Then, the measured values of αmeas and Φmeas are subtracted from the commanded values to produce αerror and Φerror in the outer loop. These error values are then fed into the Command Inverter block to be changed to rate commands, pcmd, qcmd and rcmd. The Desired Dynamics block then uses these rate commands as well as the rate measurements to create desired acceleration terms, which are favored forms of commands for the Dynamic Inversion controller.

The next block is a Dynamic Inversion Block and it produces the control surface deflection angle commands, δacmd, δrcmd and δecmd. Finally, these control surface commands are fed into the plant block, X-38 Model, via the Control Surface block. The Control Surface block includes control surface management logic, which blends the three command values, δacmd ,δrcmd, and δecmd, into two command values, δEL cmd and δr cmd, which include the dynamics of the actuators as well as the position and rate limits of the actuators.

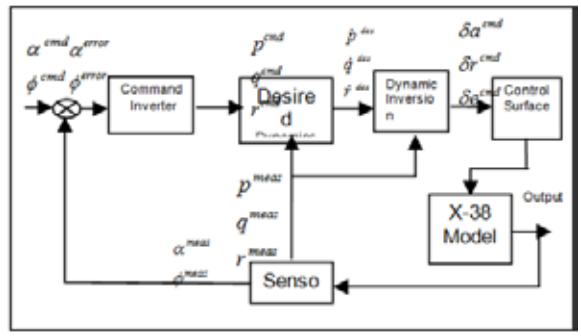

Figure. 3: Overall Dynamic Inversion Controller.

Lateral-directional DI control equations are previously developed. The following form, which is provided in Eq.10, is used during the inversion process.

$$\begin{bmatrix}\delta a\\ \delta r\end{bmatrix}^{cmd}=\begin{bmatrix}L_{\delta a} & L_{\delta r}\\ N_{\delta a} & N_{\delta r}\end{bmatrix}^{-1}\left\{\begin{bmatrix}\dot{p}\\ \dot{r}\end{bmatrix}^{des}-\begin{bmatrix}L_p & L_r & L_\beta\\ N_p & N_r & N_\beta\end{bmatrix}\begin{bmatrix}p\\ r\\ \beta\end{bmatrix}^{meas}\right\} \quad (12)$$

SIMULATION RESULT

Figure. 4 shows the simulation block diagram involving X-38 spacecraft model with actuators and the LQG controller.

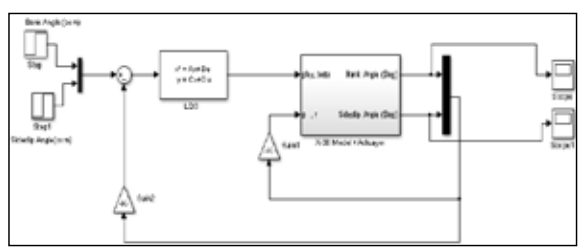

Figure. 4: Simulation block diagram for System (Plant +Actuator) with LQG Controller.

The simulation results for 10 degrees of Bank Angle and zero Sideslip Angle inputs shows unstable of outputs of system as in Figure. 5.

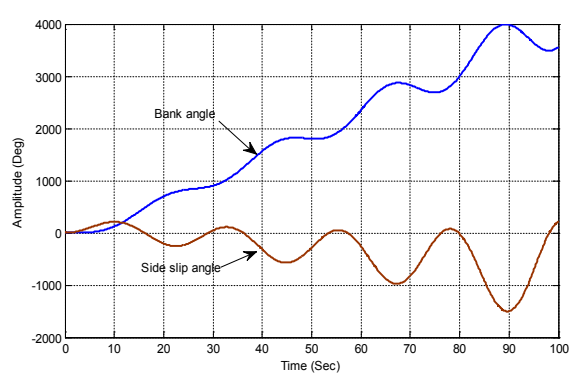

Figure. 5: X-38 model with LQG System response for 10 (Deg) Bank Angle and zero Sideslip Angle inputs.

The simulation block diagram for Augmented System (Plant +Actuator + DI) as in Figure. 6.

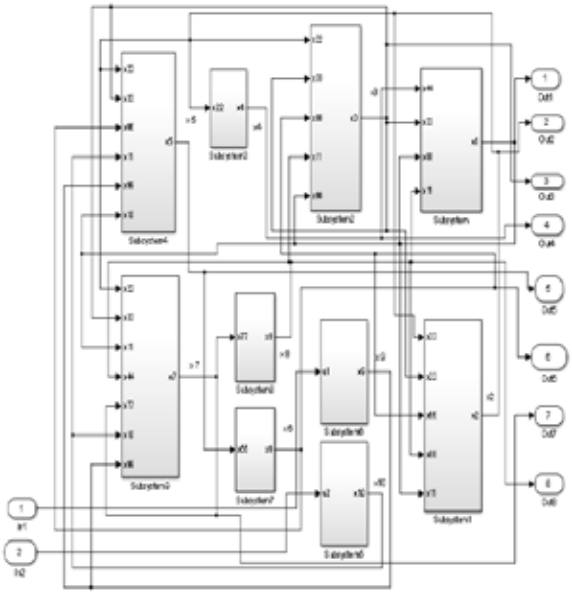

Figure. 6: Augmented System Block Diagram.

Figure. 7 shows the simulation block diagram for all desired dynamics. To satisfy the desired requirement of both time domain and frequency domain. The optimal K. is 0.08, by trial and error with LQG Controller. Figure. 8 illustrates the singular value plot of the system. The behavior of the system in the low frequency region is as desirable.

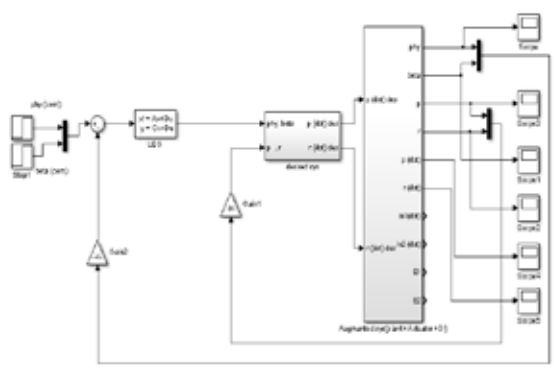

Figure. 7: Simulation Block diagram for all controlled system.

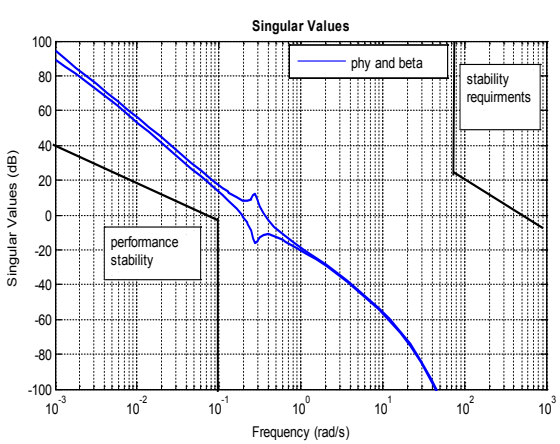

Figure. 8. The singular value plot for the controllable system with proportional desired dynamics.

Figure. 9 and 10 illustrate the step response of the 10 input to the bank angle channel and zero to the sideslip channel. The responses satisfy the time domain requirements (stable).

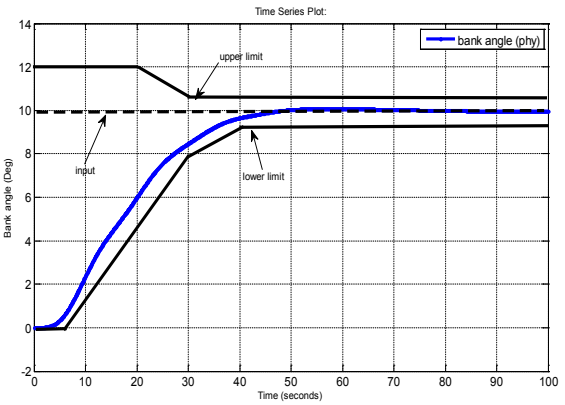

Figure. 9. The step response of the bank angle (Φ) with desired dynamics

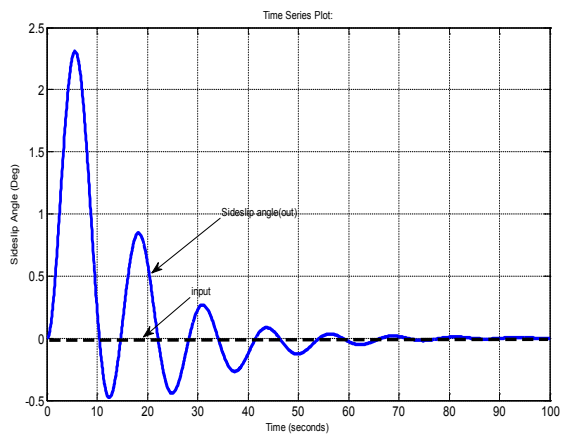

Figure. 10: The sideslip angle (β) due to step input with desired dynamics.

CONCLUSIONS

In this work, a new control schemes based on the dynamic inverse principle has been proposed for a proto type x-38 vehicle subject to certain constraints in time and frequency domain. The task for the proposed controller is to maintain zero sideslip angles while tracking a 100 bank angle. The system with dynamic inverse controller cannot satisfy the low frequency requirement. So, the system was augmented by adding one integral at each channel to overcome this problem. The sigma plot shown in Figure. 8 shows that the low frequency requirement has been satisfied. Due to inexact cancellation when using dynamic inverse technique, a linear quadratic gaussion controller has been added so as to obtain a robust system. The step response of the system with LQG is shown in Figure.s 9 and 10. It can be seen that the system satisfy the time domain requirements. The bank angle reaches its steady state value in only 45 second keeping zero sideslip angle. However, the aileron and rudder deflection limits was violated. Finally, a desired dynamic has been added to get suitable response with acceptable aileron and rudder deflection.

Volume : 3 | Issue : 5 | May 2014 • ISSN No 2277 - 8179

REFERENCE

[1] KRENER A J. "On the Equivalence of Control Systems and Linearization of Nonlinear Systems," SIAM Journal of Control and Optimization, Vol. 11, 1973, pp. 670-676. | [2] Brockett R. "Feedback Invariants for Nonlinear Systems," Proceedings of VII IFAC Congress, Helsinki, Finland, 1978, pp. 1115-1120. | [3] Falb PL and Wolovich, W."Decoupling in the Design and Synthesis of Multivariable Control Systems," IEEE Transactions of Automatic Control, AC-12, Vol. 6, 1967, pp. 651-659. | [4] Singh S and Rugh, W. "Decoupling in a Class of Nonlinear Systems by State Variable Feedback," Transactions of ASME Journal of Dynamic Systems Measurements and Control, Vol. 94, 1972, pp. 323-329. | [5] Isidori A, Krener A, Giorgi C, and Monaco S. "Nonlinear Decoupling Via Feedback: a Differential Geometry Approach," IEEE Transactions of Automatic Control, AC- 26, 1981, pp. 331-345. | [6] Cheong J, Cho Y, IkLee S."Invariant slow manifold approach for exact dynamic inversion of singularly perturbed linear mechanical systems with admissible output constraints". Journal of Sound and Vibration, 2012, pp.3710–3720. | [7] Balas G, Garrard W and Reiner J. "Robust Dynamic Inversion Control Laws for Aircraft Control", AIAA Paper 92-4329, Proceedings of the AIAA Guidance, Navigation and Control Conference, Hilton Head Island, SC, Aug. 1992, pp. 192-205. | [8] Simon C, Jonathan P, and David W. "Experimental Comparison of RobustH2 Control Techniques for Uncertain Structural Systems" Massachusetts Institute of Technology, Cambridge, Massachusetts 02139, J. GUIDANCE, VOL. 20, NO. 3, 2001 | [9] Aaron J and Barton J. "Force and Moment Approach for Achievable Dynamics Using Nonlinear Dynamic Inversion" NASA Langley Research Center Hampton, VA AIAA-1999-4001 | [10] Ito D. and Valasek, J. "Robust Dynamic Inversion Controller Design and Analysis to the X-38 Vehicle," AIAA Paper 2001-4380, AIAA Guidance, Navigation and Control Conference, Montreal, Canada, Aug. 2001. | [11] Honeywell Technology Center and Houston Engineering Center, "Application of MACH to X-38 Drop Test Vehicle," HTC Contract Number 7028327, for NASA Johnson Space Center, June 1997. |